

## Controlled Synthesis and Photoluminescent Properties of Cu<sub>2</sub>O Microcrystals with Different Morphologies

Zengming Qin,<sup>1</sup> Baibin Zhou,\*<sup>1</sup> Yongkui Yin,<sup>2</sup> and Yuzeng Sun\*<sup>3</sup>

<sup>1</sup>Key Laboratory of Design and Synthesis of Functional Materials and Green Catalysis, Colleges of Heilongjiang Province, Harbin Normal University, Harbin 150025, P. R. China

<sup>2</sup>Experimental Center of School of Public Health, Mudanjiang Medical University, Mudanjiang 157011, P. R. China

<sup>3</sup>College of Chemistry and Molecular Engineering, Peking University, Beijing 100871, P. R. China

(Received May 2, 2011; CL-110369; E-mail: bbzhou@hrbnu.edu.cn, yuzengsun@pku.edu.cn)

Cu<sub>2</sub>O microcrystals with cubic, spherical, and octahedral morphologies were easily synthesized in aqueous solution under the assistance of ultrasonic irradiation. The obtained products were characterized by using X-ray power diffractometry (XRD) and field emission scanning electronic microscopy (FE-SEM). The morphologies of Cu<sub>2</sub>O microcrystals could be controlled by simply adjusting NaOH concentration. It is believed that the difference in the growth rate of Cu<sub>2</sub>O crystal facets led to the formation of different morphologies of microcrystals, which exhibited good room-temperature photoluminescence properties with new green emission peaks at 530 nm, making them have potential applications as phosphors and biolabels.

Cu<sub>2</sub>O is an important p-type semiconductor with a direct band gap of about 2 eV.<sup>1</sup> It has unique optical properties<sup>2–7</sup> and potential applications in various fields,<sup>8–14</sup> such as solar energy conversion,<sup>8</sup> sensors,<sup>9</sup> photocatalysis,<sup>10</sup> magnetic storage,<sup>11</sup> superconductors,<sup>12</sup> CO oxidation,<sup>13</sup> and negative electrode materials.<sup>14</sup> Many efforts have been devoted to preparing different morphologies of Cu<sub>2</sub>O nanostructures or microstructures.<sup>15–20</sup> Wang et al. have synthesized Cu<sub>2</sub>O nanocubes by annealing a copper grid at 300 °C in air.<sup>15</sup> Gou and coauthors have fabricated Cu<sub>2</sub>O nanostructures through a simple solution process in the presence of CTAB.<sup>16</sup> Wu et al. have obtained Cu<sub>2</sub>O polyhedral micro/nanocrystals with amphiphilic polyvinylacetone.<sup>17</sup> Liu et al. have prepared Cu<sub>2</sub>O crystals using galvanic deposition.<sup>18</sup> Jimenez-Cadena and coauthors have obtained Cu<sub>2</sub>O bipyramid nanostructures in aqueous solution using hydrazine as a reducing agent.<sup>19</sup> Zhang's group has designed a multiple emulsion (O/W/O) system to fabricate Cu<sub>2</sub>O double tower-tip-like microstructures.<sup>20</sup> However, their photoluminescent (PL) behaviors were seldom investigated, to obtain Cu<sub>2</sub>O microcrystals with a simple method and good PL properties are still needed. In this letter, we report the synthesis of Cu<sub>2</sub>O microcrystals with cubic, spherical, and octahedral morphologies by a simple free-surfactant aqueous route under ultrasonic irradiation. All Cu<sub>2</sub>O microstructures exhibited good room-temperature PL emission properties.

In a typical synthesis, 25 mL of 0.4 mmol aqueous CuCl<sub>2</sub> solution was added dropwise to an identical volume of aqueous NaOH solution with various concentrations under continuous magnetic stirring. 20 mL of 1 mmol aqueous ascorbic acid solution was rapidly mixed with the above solution. The resulting solution was ultrasonicated for 60 min. Finally, the products were collected, washed several times with distilled water and absolute ethanol, and characterized by using XRD

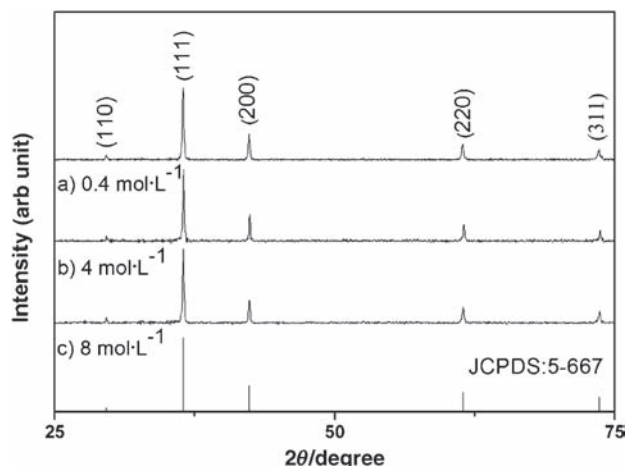


**Figure 1.** XRD patterns of Cu<sub>2</sub>O microcrystals obtained at different initial NaOH concentrations.

(Bruker D8 with Cu K $\alpha$  radiation), FE-SEM (Hitachi S-4800), and PL (Perkin-Elmer LS 55).

As shown in Figure 1, all diffraction peaks can be indexed to the pure cubic phase of Cu<sub>2</sub>O. No other peaks from impurities have been detected in the synthesized products. Figure 2 shows SEM images of typical products obtained at different NaOH concentrations and indicate that large quantity and good uniformity were achieved by using this approach. While NaOH concentrations were gradually increased, the microcrystal morphologies can be tuned from cubic to spherical and then to octahedral, with the edge length, the average diameter, and the axis size of 0.67, 0.99, and 1.12  $\mu\text{m}$ , respectively. The insets are corresponding high-resolution SEM images, which clearly confirm the successful synthesis of cubic, spherical, and octahedral microcrystals.

It could be explained that the morphologies evolution of Cu<sub>2</sub>O microcrystals was a result of different growth rate of crystal facets. The crystal facets with higher growth rate will be first eliminated, and the crystal morphologies were defined by the crystal facets of slower growth rate. At low 0.4 mol L<sup>-1</sup> NaOH concentration (pH  $\approx$  13.1), the microcubes bounded by {100} and {111} facets were easily obtained, which might be partially attributed to its own growth habit.<sup>16</sup> With the use of 4.0 mol L<sup>-1</sup> NaOH (pH  $\approx$  14.1), the microcubes evolved into microspheres due to indistinguishable growth rate of {100} and {111} facets. After NaOH concentration was increased to 8.0 mol L<sup>-1</sup> (pH  $\approx$  14.4), octahedral microcrystals were formed because of the high growth rate of {100} planes and the low

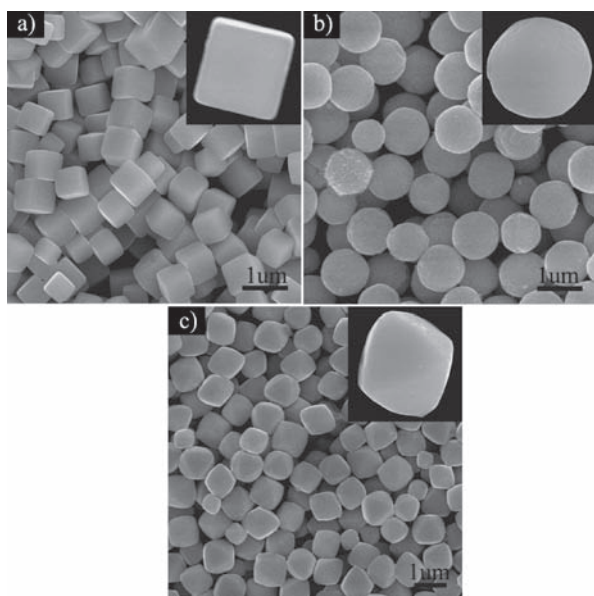


**Figure 2.** SEM images of  $\text{Cu}_2\text{O}$  microcrystals obtained at different initial NaOH concentrations: (a) 0.4, (b) 4.0, and (c) 8.0 mol  $\text{L}^{-1}$ . The insets are corresponding high-resolution SEM images.

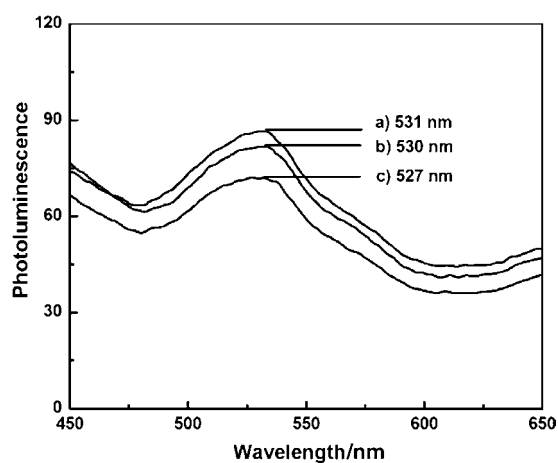


**Figure 3.** Room-temperature PL spectra of  $\text{Cu}_2\text{O}$  microcrystals: (a) cubic, (b) spherical, and (c) octahedral.

growth rate of  $\{111\}$  facets. The above results could be attributed to that the change of adsorption behavior of  $\text{Cl}^-$  and  $\text{OH}^-$  to some crystal facets leading to the difference in growth rate of crystal facets and, therefore, the formation of microcrystals with various morphologies.

The room-temperature PL spectra of the products are shown in Figure 3. With excitation at 360 nm,  $\text{Cu}_2\text{O}$  microstructures show a broad green emission peak at ca. 531 nm. The emission peak positions are different from other previously reported  $\text{Cu}_2\text{O}$  nanostructures and microstructures,<sup>2–6</sup> such as 560 nm,<sup>2</sup> 525 nm,<sup>3</sup>

493 nm,<sup>4</sup> 484 nm,<sup>5</sup> and 436 nm.<sup>6</sup> The peaks show a blue shift when compared with the bulk  $\text{Cu}_2\text{O}$  (570 nm), which might originate from the quantum confinement effects.<sup>6</sup> The PL intensity of microcubes is stronger than that of spherical and octahedral microcrystals. The PL intensities exhibit great dependence on morphologies and sizes of the samples, which is consistent with formerly reported  $\text{Cu}_2\text{O}$  nanostructures.<sup>3</sup> The true factors influencing PL properties are still not clear to need further investigation.

$\text{Cu}_2\text{O}$  microcrystals with cubic, spherical, and octahedral morphologies have been easily synthesized by a simple aqueous solution route under ultrasonic irradiation. The morphologies of  $\text{Cu}_2\text{O}$  microcrystals can be controlled by adjusting NaOH concentration. All microcrystals exhibit good photoluminescence properties, and they might have potential applications as phosphors and biolabels.

The work was supported by NSFC (Nos. 20671026 and 20971032).

## References

- 1 Y. Yu, F.-P. Du, J. C. Yu, Y.-Y. Zhuang, P.-K. Wong, *J. Solid State Chem.* **2004**, *177*, 4640.
- 2 S. Lv, H. Suo, C. Wang, S. Jing, T. Zhou, Y. Xu, J. Wang, C. Zhao, *Solid State Commun.* **2009**, *149*, 404.
- 3 G. S. Hsiao, M. G. Anderson, S. Gorer, D. Harris, R. M. Penner, *J. Am. Chem. Soc.* **1997**, *119*, 1439.
- 4 Z. Yang, C.-K. Chiang, H.-T. Chang, *Nanotechnology* **2008**, *19*, 025604.
- 5 M. Zahmakıran, S. Özkır, T. Kodaira, T. Shiomi, *Mater. Lett.* **2009**, *63*, 400.
- 6 Y. Xu, D. Chen, X. Jiao, K. Xue, *J. Phys. Chem. C* **2007**, *111*, 16284.
- 7 S. Jana, P. K. Biswas, *Mater. Lett.* **1997**, *32*, 263.
- 8 R. N. Briskman, *Sol. Energy Mater. Sol. Cells* **1992**, *27*, 361.
- 9 J. Zhang, J. Liu, Q. Peng, X. Wang, Y. Li, *Chem. Mater.* **2006**, *18*, 867.
- 10 H. Yu, J. Yu, S. Liu, S. Mann, *Chem. Mater.* **2007**, *19*, 4327.
- 11 X. Li, H. Gao, C. J. Murphy, L. Gou, *Nano Lett.* **2004**, *4*, 1903.
- 12 E. W. Bohannon, M. G. Shumsky, J. A. Switzer, *Chem. Mater.* **1999**, *11*, 2289.
- 13 B. White, M. Yin, A. Hall, D. Le, S. Stolbov, T. Rahman, N. Turro, S. O'Brien, *Nano Lett.* **2006**, *6*, 2095.
- 14 P. Poizot, S. Laruelle, S. Grugeon, L. Dupont, J.-M. Tarascon, *Nature* **2000**, *407*, 496.
- 15 Y. Q. Wang, W. S. Liang, A. Satti, K. Nikitin, *J. Cryst. Growth* **2010**, *312*, 1605.
- 16 L. Gou, C. J. Murphy, *Nano Lett.* **2003**, *3*, 231.
- 17 W.-T. Wu, L. Shi, Q. Zhu, Y. Wang, G. Xu, W. Pang, F. Lu, *Chem. Lett.* **2006**, *35*, 574.
- 18 G. Liu, L. Wang, D. Xue, *Mater. Lett.* **2010**, *64*, 2475.
- 19 G. Jimenez-Cadena, E. Comini, M. Ferroni, G. Sberveglieri, *Mater. Lett.* **2010**, *64*, 469.
- 20 H. Zhang, X. Zhang, H. Li, Z. Qu, S. Fan, M. Ji, *Cryst. Growth Des.* **2007**, *7*, 820.